Accepted Manuscript

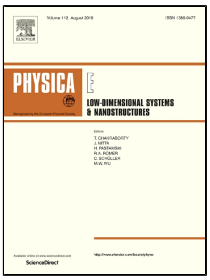

Density Functional Theory model for carbon dot surfaces and their interaction with silver nanoparticles

R.E. Ambrusi, J.M. Arroyave, M.E. Centurión, M.S. Di Nezio, M.F. Pistonesi, A. Juan, M.E. Pronsato

PII:	S1386-9477(19)30713-1
DOI:	10.1016/j.physe.2019.113640
Article Number:	113640
Reference:	PHYSE 113640
To appear in:	*Physica E: Low-dimensional Systems and Nanostructures*
Received Date:	13 May 2019
Accepted Date:	16 July 2019

Please cite this article as: R.E. Ambrusi, J.M. Arroyave, M.E. Centurión, M.S. Di Nezio, M.F. Pistonesi, A. Juan, M.E. Pronsato, Density Functional Theory model for carbon dot surfaces and their interaction with silver nanoparticles, *Physica E: Low-dimensional Systems and Nanostructures* (2019), doi: 10.1016/j.physe.2019.113640

Density Functional Theory model for carbon dot surfaces and their interaction with silver nanoparticles

R.E. Ambrusi[1,3], J.M. Arroyave[2,4], M.E. Centurión[2,4], M.S. Di Nezio[2,4], M.F. Pistonesi[2,4], A. Juan[1,3], M.E. Pronsato[1,3,*].

[1] Instituto de Física del Sur (IFISUR), CONICET, Av. L. N. Alem 1253, B8000CPB-Bahía Blanca, Argentina.

[2] Instituto Química del Sur (INQUISUR), CONICET, Av. L. N. Alem 1253, B8000CPB-Bahía Blanca, Argentina.

[3] Departamento de Física, Universidad Nacional del Sur (UNS), Av. L. N. Alem 1253, B8000CPB-Bahía Blanca, Argentina.

[4] Departamento de Química, Universidad Nacional del Sur (UNS), Av. L. N. Alem 1253, B8000CPB-Bahía Blanca, Argentina.

***Corresponding Author**

E-mail: **pronsato@criba.edu.ar**

Tel-Fax: 54 291 4595142.

Abstract

Density functional theory (DFT) and time dependent density functional theory (TDDFT) calculations were performed to represent carbon dots surfaces. The addition of different oxygen functional groups to the aromatic carbon core structure and the stability in the interaction with silver nanoparticles was also investigated. Adsorption energies were evaluated in order to compare the competition for adsorption sites on silver surface with D-glucose and D-gluconate ion molecules. The -COOH and -COO groups and the interaction of the latter with silver were proposed to explain some features of the UV-visible absorption spectra, which could also contribute to an explanation for the charge observed on carbon dot surfaces.

Keywords

carbon dots, silver nanoparticles, UV-visible spectra, DFT, adsorption energy

1. Introduction

Graphene quantum dots (GQDs) are graphenes with finite size, which can be fabricated by bottom-up and top-down synthesis approaches [1,2]. Several theoretical studies were already performed studying the electronic and optical properties of GQDs [3-7], analyzing the influence of size, shape, functional groups and gas adsorption on electronic and optical properties.

On the other hand, carbon dots (C-dots) are basically carbon nanoparticles with size below 10 nm [8]. Synthesis of C-dots is made possible in multiple ways including top-down approaches as arc discharge, laser ablation, electrochemical oxidation, or bottom-up approaches as combustion, template, hydrothermal, ultrasonic, microwave, and solvothermal processes [9]. Many experimental approaches investigate its applications due to their fascinating optical properties, such as photoluminescence, photoinduced electron transfer, chemiluminescence, and electrochemiluminescence [10-13]. Nevertheless not many theoretical attempts have been performed in order to have a reliable representation of this type of structures, and classical corone model to describe its properties do not have a suitable absorption behavior in the UV-visible region [5].

In addition combinations of C-dots and silver nanoparticles (AgNP) have been recently synthesized and applied in different devices. In this sense, C-dots/silver nanocomposites were prepared by hydrothermal treatment of ascorbic acid and were applied for detecting iodide ions using the fluorescence of these structures in aqueous media [14]. Also AgNPs supported on C-dots derived from biomass as a combined reducing and capping agent for electrocatalytic applications [15]. Glucose detection based on C-dots supported on AgNPs represents a new example of wide application of C-dots [16]. Silver nanoclusters supported on C-dots were synthesized through a facile and green approach with only glucose and $AgNO_3$ as precursors with remarkable electrocatalytic performance towards oxygen reduction with the most efficient four-electron transfer process [17]. The design of a fluorometric and colorimetric dual-signal sensor for H_2O_2–assisted glucose detection based on Au@Ag NPs and C-dots was achieved [18]. Carbon quantum dots (CQDs) decorated Ag nanoparticles (Ag@CQDs) were successfully synthesized and characterized by UV-Vis spectroscopy,

fluorescence, FT-IR, and transmission electron microscopy (TEM), then utilized for the sensitive detection of chloride ions (Cl^-) [19]. For that reason, a reliable model of C-dots to evaluate and understand the interaction of C-dots with other structures like AgNPs would be very helpful for future experiments in the field.

The formation of AgNPs by glucose were reported by González Fá et. al. [20], and the role of D-glucose and D-gluconate ion acting as capping agents on AgNPs was evaluated using both Raman and DFT studies [21].In addition, the synthesis of C-dots from hydrocarbons like glucose as a source of carbon is also possible applying hydrothermal methods or microwaves [12,22]. For that reason a theoretical representation of these structures in aqueous media would be very helpful to interpret experimental results or to the design of new experiences. In the present work, we provide the bases of construction of a reliable model to represent C-dots surfaces using simple structures. We also reproduce the UV-visible spectra behavior for different oxygen containing groups with good quality.

2. Theoretical model

DFT and TDDFT calculations were performed using the Vienna Ab initio Simulation Package (VASP) [23,24], which employs a plane-wave basis set and a periodic supercell method. The generalized gradient corrected approximation (GGA) functional of Perdew, Burke, and Ernzerhof (PBE) was used [25]. The Kohn–Sham equations were solved variationally using the projector- augmented-wave (PAW) method [26,27]. For the plane-wave basis set expansion a cutoff energy of 400 eV was used, overall with the gamma-centered Monkhorst–Pack scheme [28] with 1x1x1 k-points grid for the integration over the Brillouin zone. A Gaussian smearing approach was used for the electronic states partial occupations near the Fermi level, with a 0.2 eV smearing width.

Geometry optimizations were obtained by minimizing the total energy of the supercell using a conjugated gradient algorithm to relax ions [29], until it converged within 10^{-4} eV and the forces on each ion were less than 0.01 eV $°A^{-1}$. The Grimme's DFT-D2 method was adopted to account for the van der Waals interactions (vdW), which is optimized for several DFT functionals [30]. Then the electronic structure was obtained at B3LYP level [31] and the solvent effect was considered applying VASPsol package [32,33] for energies calculations, density of states (DOS) and partial density of states (PDOS).

All the C-dots calculations were performed in a box of 30x30x30 Å, to achieve the optimized isolated structure, as was performed in previous works following graphene quantum dots model [3,5]. To evaluate the properties of silver nanoparticles and its interactions with C-dots, the same box cell was used and a triangular silver cluster of three atoms was employed. This cluster size has demonstrated being a good approximation for adsorption of molecules on silver nanoparticles [34] and was used for calculating to the adsorption energies on glucose and gluconate ion on silver nanoparticles [21,35]. A similar model was used to obtain SERS and UV-visible spectra of silver nanoparticles [34,35]. Ag_3 cluster relaxation at PBE level lead to a bond distance of 2.73 Å which match well with other DFT calculations [34,36].

Eqn (1), was used to calculate the adsorption energy for the molecule or C-dot (E_{ads}) on the silver nanoparticle

$$E_{ads} = E(Ag_3 + molecule\ (or\ Cdot)) - E(Ag_3) - E(molecule\ (or\ Cdot)) \quad (1)$$

where E(Ag_3+molecule (or Cdot)), E(molecule (or Cdot)) and E(Ag_3) are the total energies of the molecule (D-glucose or D-gluconate) or C-dot adsorbed on Ag_3 cluster, the isolated Ag_3 cluster, and the isolated molecule or C-dot respectively. With this definition negative adsorption energy corresponds to a stable adsorption of the molecules or C-dot on the silver surface.

UV-visible absorption calculations were carried out applying TDDFT for linear optical properties implemented in VASP [37,38] at the B3LYP level including solvent effect.

3. Results and Discussion

Recent calculations studied the optical and electronic properties of graphene quantum dots with symmetrical form [5]. Different shapes and functional groups at the edges of these structures were also considered [3,4]. However, the maximum in the absorption spectrum achieved for these structures are far for the maximum obtained for C-dots synthesized by hydrothermal methods [8,9,18,39,40]. In order to achieve an adequate model to represent C-dots, different structures were proposed. In this sense, their UV-visible spectra were calculated with the aim to achieve structures with a maximum absorption peak in the region 240-300 nm [18,40], which corresponds well with the experimental measurements.

Attending to the fact that C-dots structures consist of graphitic and amorphous carbon structures and functional groups formed by the carbonization of organic molecules [39], with a carbonized core [39,41], we constructed a geometrical structure which represents well C-dot behavior at its core-surface interface. Fig. 1 shows different structures proposed to represent the C-dots carbon structure. In a realistic model, these layers could be aggregated, but for the main aim of the present work the use of single layer does not represent a problem. This is due to the interaction between nanographene layers will be van der Waals forces [42], not affecting the chemical properties of its edges. To indentify the different structures, a number at the beginning is used to indicate the number of rings followed by the letters R_h, R_diag, R_triang referring to the structures with the center of the rings in horizontal, diagonal and triangular position respectively.

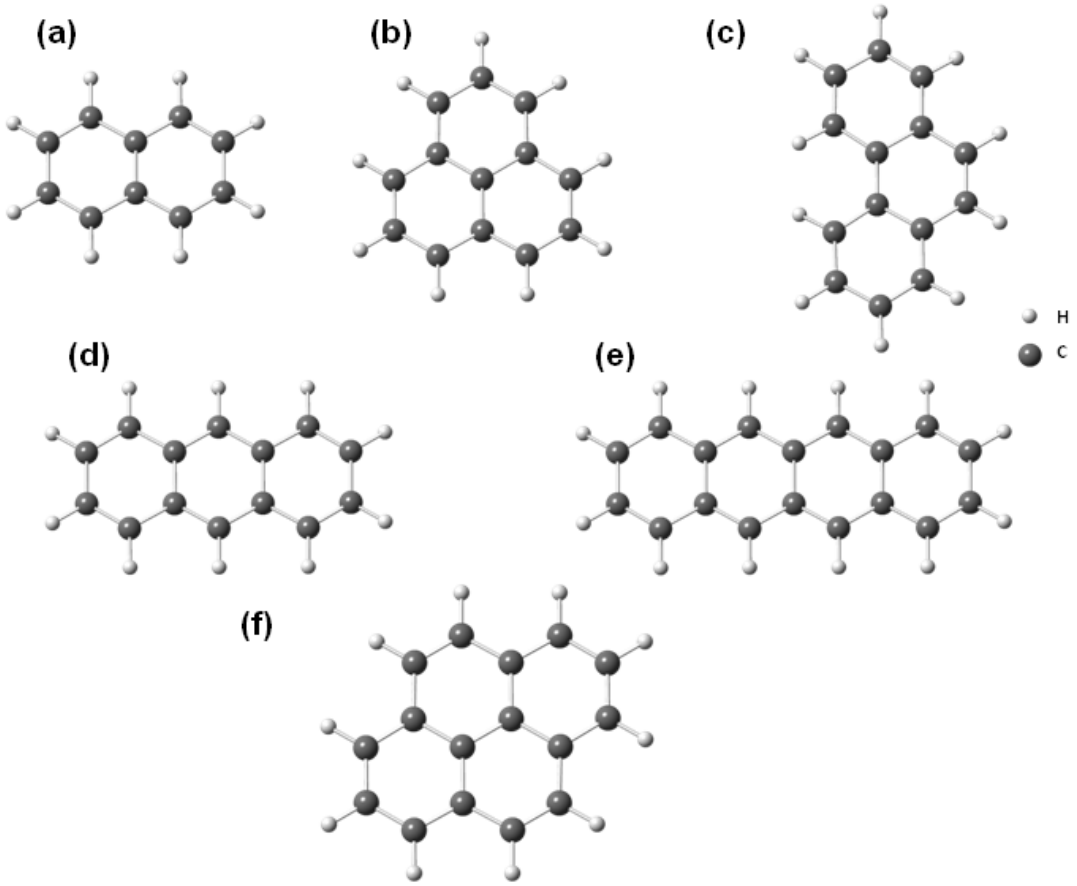

Fig. 1: Optimized geometry structures to represent C-dots without functional groups for ; (a) 2R, (b) 3R_triang, (c) 3R_diag, (d) 3R, (e) 4R and (f)4R_paralelogram.

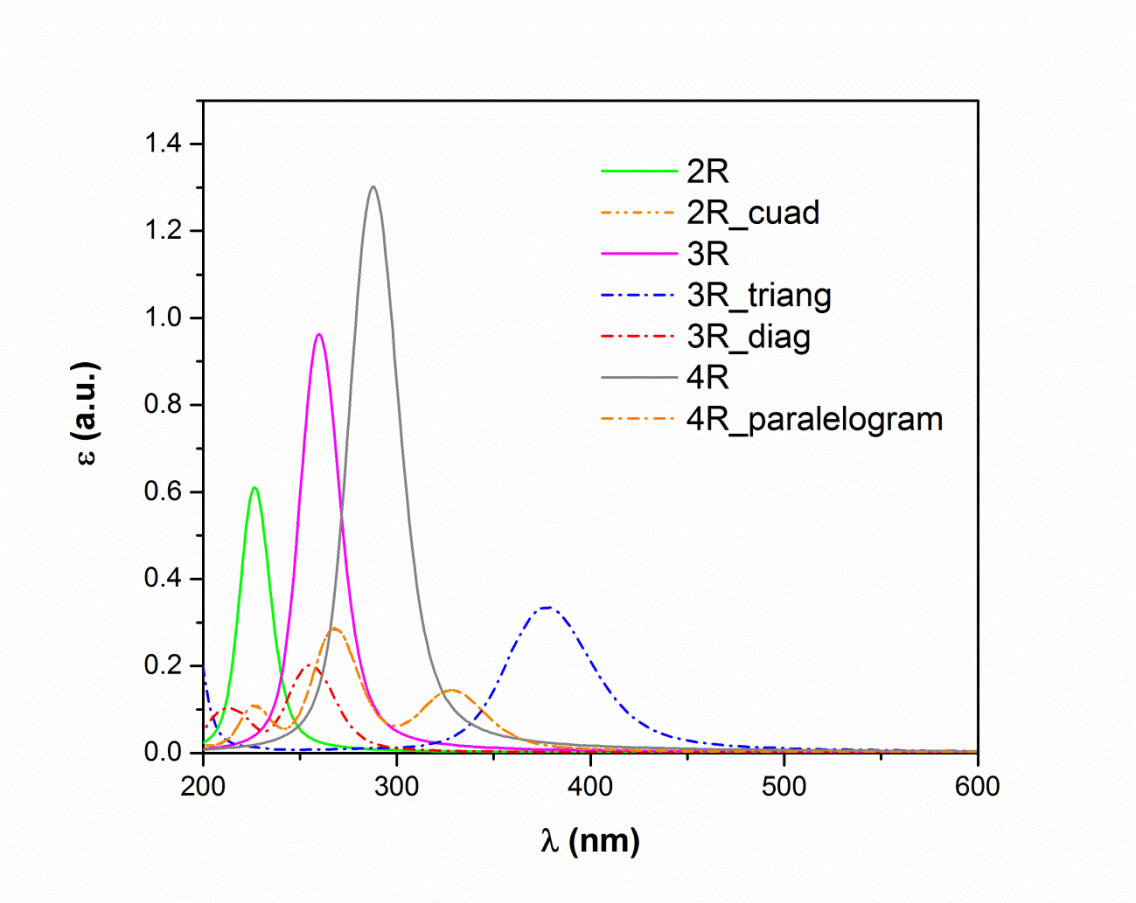

Fig. 2: Calculated optical absorption spectra for C-dots of different sizes and shapes.

The spectra obtained for different ring sizes, are shown in Fig.2. The peak at approximately 381 nm, corresponds to a three rings (3R_triang) with a number of carbon atoms that do not match with the Hückel rule for aromatic compounds [43]. Electronic and aromatic properties of nanograhene are highly dependent of its size and edge shape, determining different aromaticity patterns in the structure [44-46]. This affects band gap and electronic properties, which partially explains why the peak is shifted when not all the rings in the structure are aromatic due to different aromatic periodicity. Instead, the other proposed structures contain its maximum among approximately 220-280 nm, as expected for aromatic π systems [47].The absorption spectra represented with a dash-dotted line contain three maximums, which do not match well with the experimental ones reported for C-dots aromatic structure [8]. As the number of rings is increased, a shift of the peak to higher wave length is observed. When the Hückel rule is achieved, the aromatic absorption peak of the proposed structures is similar to the absorption bands obtained for C-dots by experimental measurements due to π-π* transition [8,39]. For that reason, chains of carbon rings are considered adequate to model the behavior of C-dots carbon structure.

As it is described in several works [18,39-41,48,49], the surface of C-dots contains different functional groups. Based on structural properties [41,48,49], typical functional groups are given by hydroxyl, carbonyl and carboxylic groups. Fig.3 shows the selected structures proposed to represent the C-dots surface, with the addition of a functional group in one extreme, associated with the surface. To identify this, we added

a number which represent the number of functional groups, followed by the typical molecular formula for the specified functional group. In this sense, the molecular formulas -OH, -COOH, -COO were used to indicate hydroxyl, carboxyl and carboxylate anion groups.

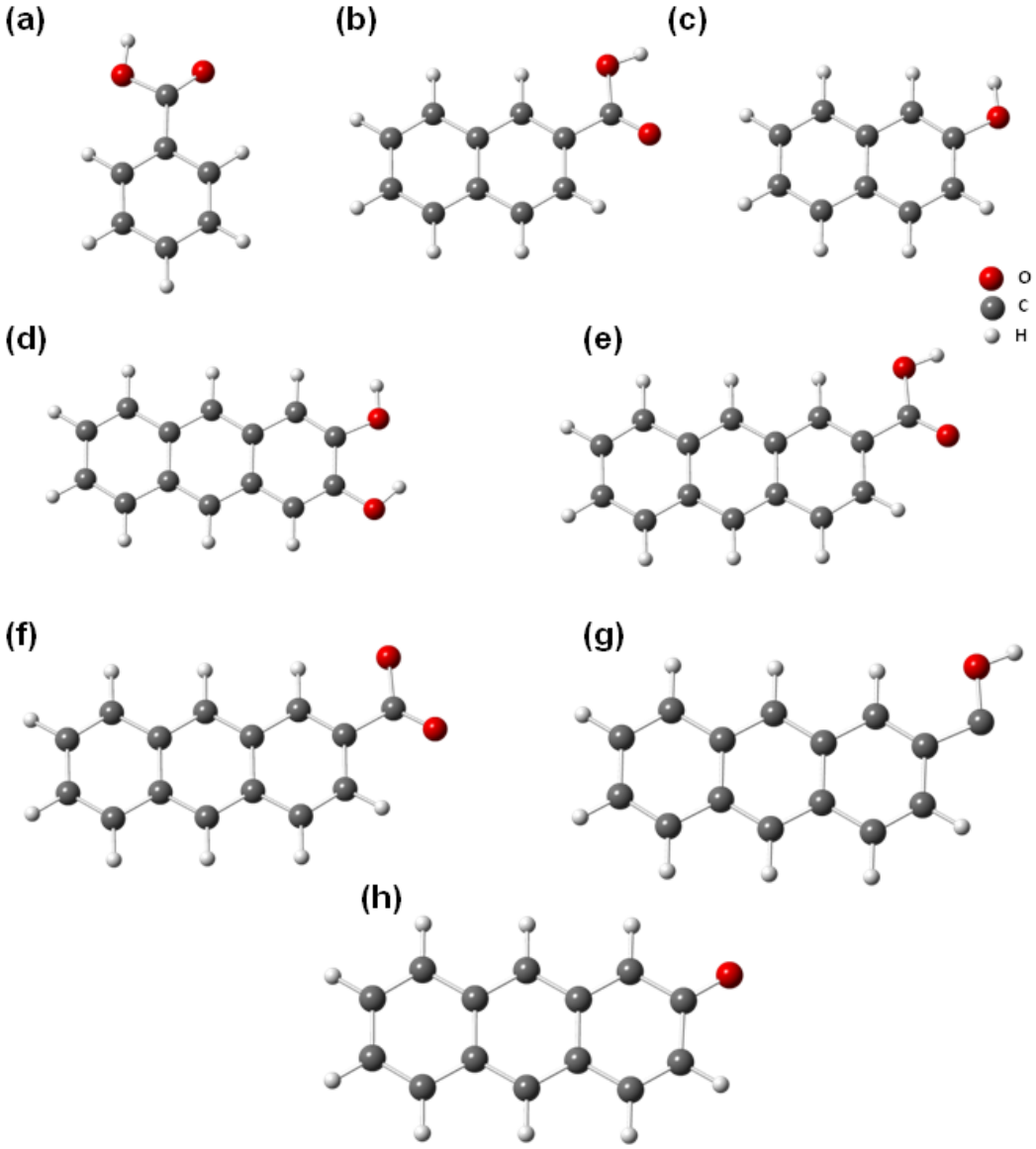

Fig. 3: Optimized geometry structures to represent C-dots with functional groups for; (a) 1R_1COOH, (b) 2R_1COOH, (c) 2R_1OH, (d) 3R_2OH, (e) 3R_1COOH, (f) 3R_1COO, (g) 3R_1C-OH, (h) 3R_1Carbonyl.

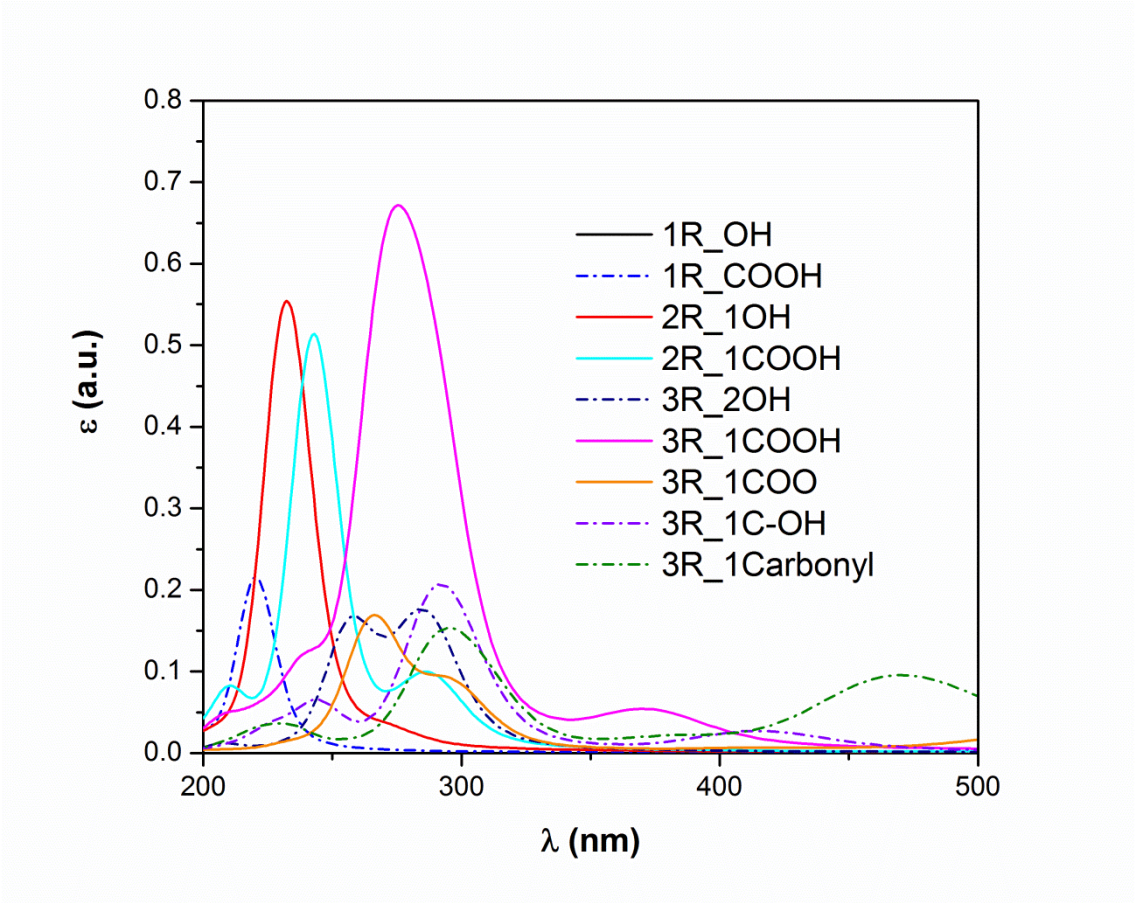

Fig. 4: Calculated optical absorption spectra for C-dots of different sizes with functional groups.

To analyze the effect of the functional groups in C-dots spectra, the resonance absorption peaks of these structures were obtained again, and are shown in Fig. 4. As can be seen, the peak associated with π-π* transitions, in all the cases is red shifted. Also, a small peak appears at higher wave lengths for almost all the structures, that depends on the functional group considered and the number of rings. This region of absorption is associated with a n-π* transition [8,39]. Since, the -COOH group can be dissociated in solution, the group -COO without H atom, was also considered to represent this situation, and included in the same graph. The spectra represented with dash-dotted lines, do not correspond well with the reported experimental data obtained for C-dots structures [8,39]. On the contrary, the ones with solid lines reproduce better the experimental behavior within some shifts of the maximum peak values, being the 3R_COOH or 3R_COO structures the most suitable. In this sense, the proposed structures can be considered basic units that constitute the C-dot surface-solution interface. These are important structures where evaluate their interaction with silver NP.

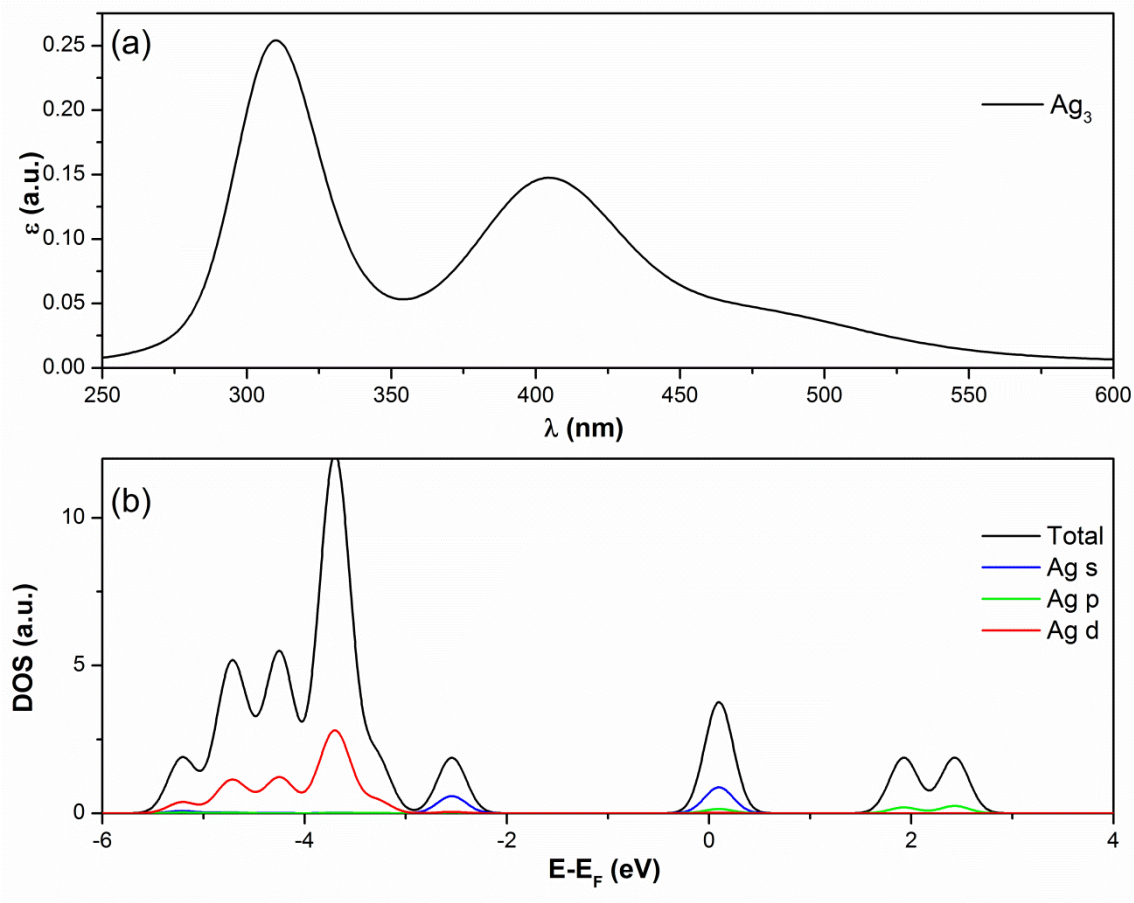

Fig. 5. Calculated, **(a)** optical absorption spectra for Ag_3 cluster, and **(b)** DOS and PDOS for Ag atom.

As can be observed in Fig. 5 (a), Ag_3 absorption spectra has two clear peaks. One at approximately 410 nm, which match very well with the silver surface peak obtained in UV-visible spectras for AgNP synthesized by glucose [20,50]. Accordingly to recent works [51,52], this peak corresponds to dipole plasmon resonance. In addition, another absorption peak is observed at approximately 314 nm. It was reported that this peak is associated with silver nanoprism structures and corresponds to quadrupole plasmon resonance [52]. In the present calculations, all these resonance peaks are related with electronic transitions [53,54], and to verify if the same are associated with dipole and quadrupole plasmon resonance, electric dipole and quadrupole transition selection rules must be fulfilled. After an analysis of DOS and PDOS for Ag_3 cluster (Fig. 5 (b)), transitions between *d* occupied states and *s* unoccupied states are possible, in agreement with a pure quadrupole transition selections rule, $\Delta l = \pm 2$, where l is the angular momentum quantum number [53], and for that reason the peak at 314 nm appears. In addition, based on PDOS, transitions between *d* and *s* occupied bands to p unoccupied bands are also possible, this corresponding to $\Delta l = \pm 1$ dipole transition selection rule. The fact that the peak at lower wave lengths is higher, contrasts with the measured UV-visible spectra, where the opposite occurs [50]. However, this behavior is attributed to the considered triangular cluster, with states that reproduce only approximately the behavior of the AgNP surface atoms.

González Fa et al. [21], reported through a correlation between Raman measurements and DFT calculations, that both D-glucose and D-gluconate ion molecules can be found adsorbed on silver surface NPs, acting as *capping* agents. In the present work, it is interesting to analyze how silver NPs interacts with C-dots in dilute systems with and without capping agents, using the mentioned molecules for capping. In the first case, taking into account a possible competition for adsorption sites between C-dots structures and D-glucose or D-gluconate ion, we also carried out calculations using the most stable configurations of these molecules [21,50]. Fig. 6 and 7 shows all the optimized structures.

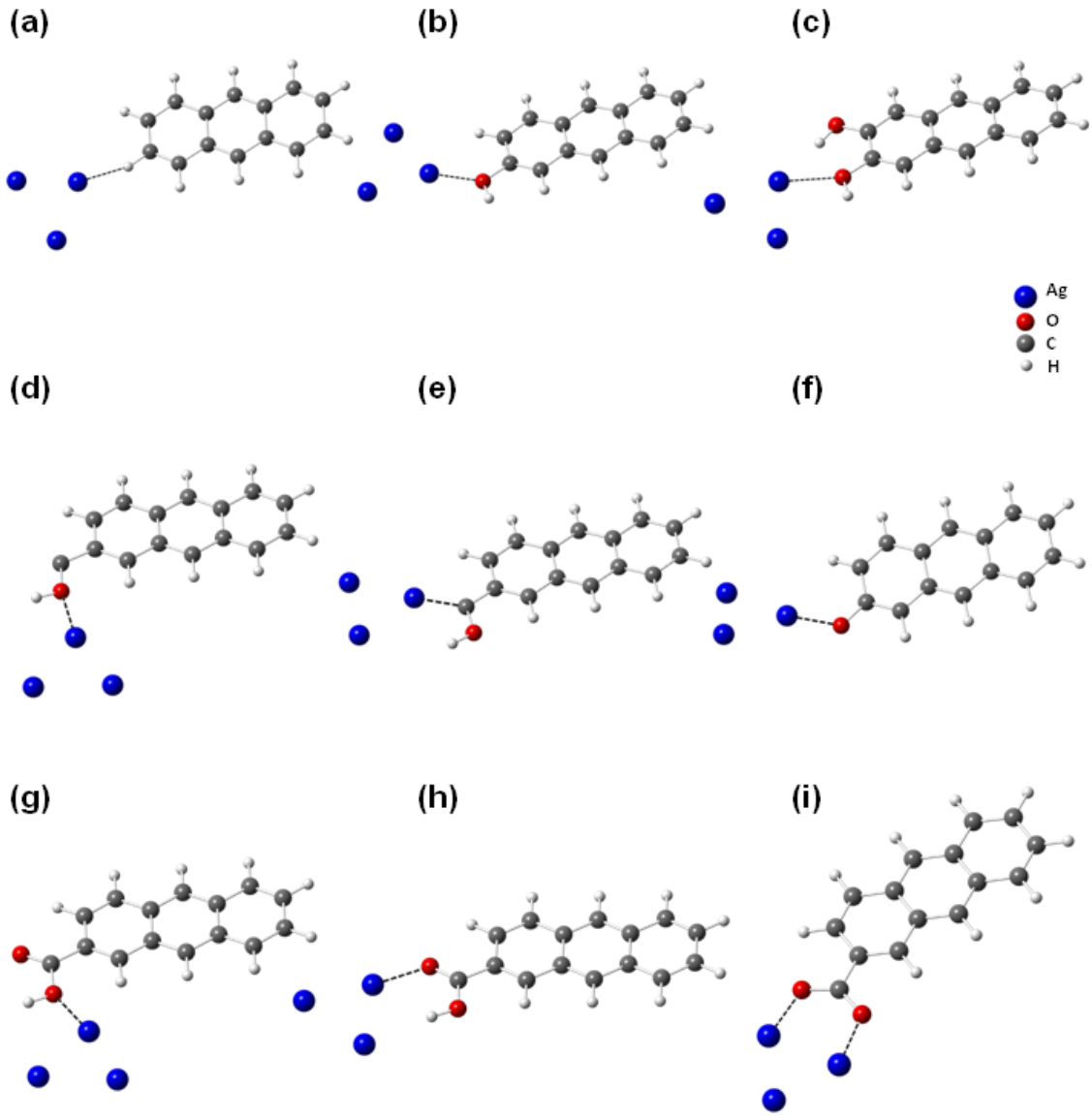

Fig. 6. Optimized geometry structures for C-dots adsorbed on Ag_3 cluster; (a) 3R_Ag_3, (b) 3R_1OH-Ag_3, (c) 3R_2OH-Ag_3, (d) 3R_1C-OH-Ag_3 (geom1), (e) 3R_1C-OH-Ag_3 (geom2), (f) 3R_1Carbonyl-Ag_3, (g) 3R_1COOH-Ag_3 (geom1), (h) 3R_1COOH-Ag_3 (geom2), (i) 3R_1COO-Ag_3.

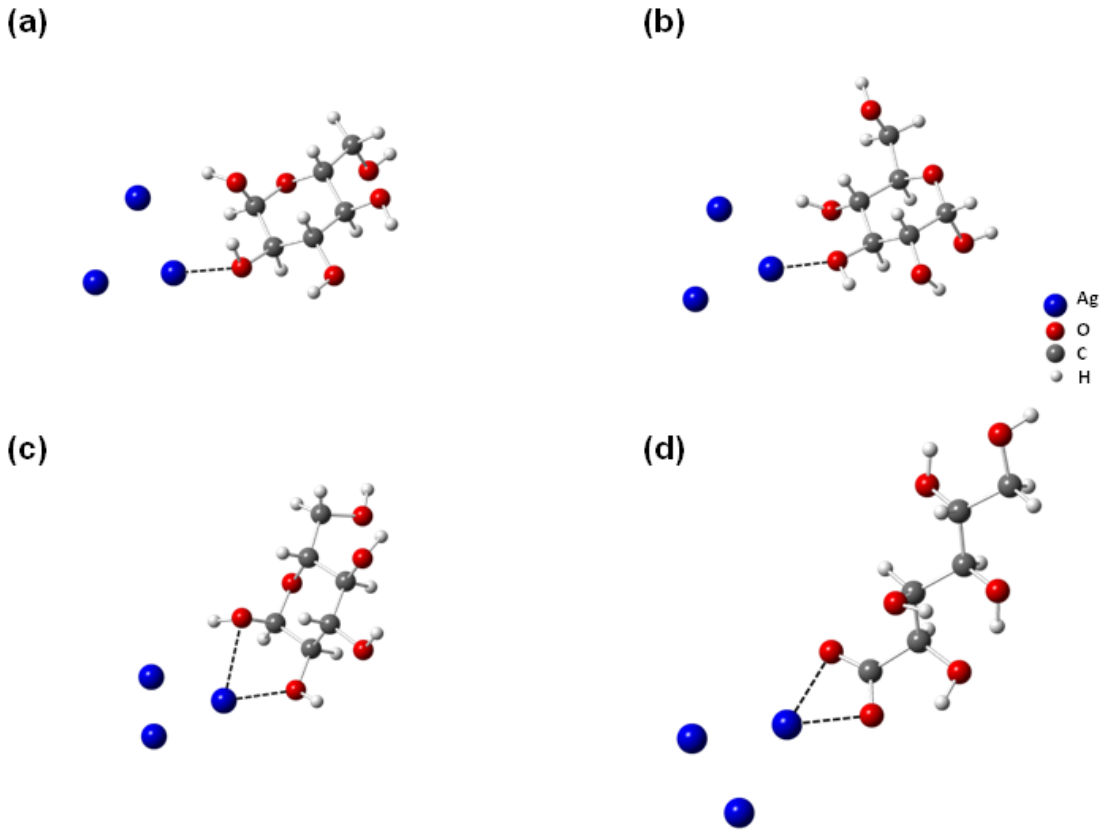

Fig. 7. Optimized geometry structures for molecules adsorbed on Ag_3 cluster; (a) α-D-glucose (geom1)-Ag_3, (b) α-D-glucose (geom2)-Ag_3, (c) α-D-glucose (geom3)-Ag_3, (d) α-D-gluconate.

Table 1. Adsorption energies and bond distances for C-dots and molecules adsorbed on Ag_3 cluster.

System	Eads/eV	d/Å
3R_Ag_3	-0.07	2.19
3R_1OH-Ag_3	-0.38	2.36
3R_2OH-Ag_3	-0.15	2.47
3R_1C-OH-Ag_3 (geom1)	-0.12	2.52
3R_1C-OH-Ag_3 (geom2)	-1.76	2.11
3R_1Carbonyl-Ag_3	-2.74	2.10
3R_1COOH-Ag_3 (geom1)	-0.18	2.38
3R_1COOH-Ag_3 (geom2)	-0.37	2.24
3R_1COO-Ag_3	-3.98	2.21
α-D-glucose-Ag_3 (geom 1)	-0.40	2.39
α-D-glucose-Ag_3 (geom 2)	-0.52	2.31
α-D-glucose-Ag_3 (geom 3)	-0.44	2.36
D-gluconate	-5.19	2.30

Table 1, reports the adsorption energies and bond distances, indicated with a black dotted line in Fig. 6 and 7, between interacting atoms for the different C-dots

structures and molecules adsorbed on a silver Ag_3 cluster. The less stable interaction occurs between Ag and H atoms at the Ag_3 cluster. C-dots with -OH surface groups are stable on Ag_3 cluster, but these groups do not interact strongly enough with silver to produce the displacement of D-glucose or D-gluconate ion. The same occur for –COOH. In the case of -C-OH (geom2) and carbonyl groups, they are stable enough to replace D-glucose, however their absorption peaks do not match very well with the experimental ones as was already analyzed in Fig. 4. A change occurs with -COO group. Compared the C-dot adsorption for –COOH and -COO groups, the adsorption on silver is more stable for –COO group, consequently it is expected that the –COOH groups have a major tendency to dissociate when they are adsorbed on Ag_3 cluster. Moreover, the adsorption energy is more than 3.5 eV higher in absolute value than D-glucose in its more stable configuration, which means that an exchange between D-glucose and C-dot is energetically favorable. From this results, it is possible to suggest that, even in a stage where AgNPs are adsorbed with D-glucose and D-gluconate as capping agents, the interaction between AgNPs and C-dots can be produced directly between C-dot and silver on free sites, and also by the replacement of D-glucose by C-dot structures on the silver surface adsorption sites occupied by this molecule. If the adsorption of C-dots through –COOH or –COO groups can occur as calculations suggest, this phenomenon could explain negative charge (z potentials) surrounding C-dots, which is observed in the characterization of their experimental synthesis [8]. Since, the source of this charge can be then attributed to the $–COO^-$ anion, which is feasible based on the correlation between experimental and calculated spectra when this group is present.

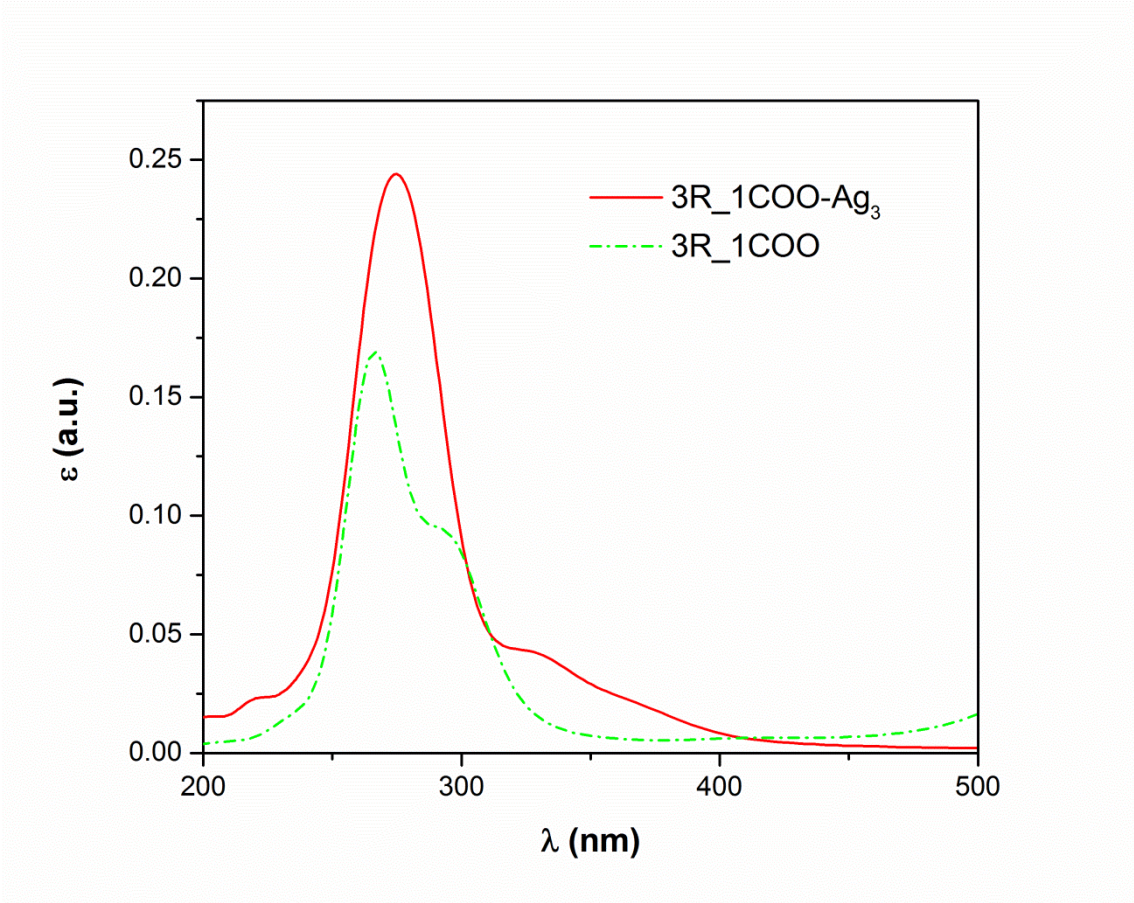

Fig. 8. UV-visible spectra of C-dot(ads)+Ag_3 and C-dot isolated, both with -COO group.

Among the different oxygenated groups studied on the C-dot surface model, the -COO group is the one which is adsorbed more strongly on the silver surface model. For that reason, it is interesting to analyze its spectra in order to describe C-dot general characteristics when it is adsorbed. Fig. 8, shows the spectra corresponding to C-dot with -COO group, adsorbed on a silver cluster. In addition, we included the spectra of the isolated C-dot for comparison (dash-dotted line). An intensification of the aromatic peak occurs after the interaction with silver. Also, the two peaks of silver disappear, and a round small peak is observed at approximately 335 nm, which could be associated with the small shoulder peak in isolated C-dots shifted. This is probable due to transitions corresponding to O-Ag bonds states near the Fermi level, which yield to a red shift of the wave length.

4. Conclusions

A suitable model for representation of C-dots and its interactions with AgNPs, which predicts well aromatic and functional groups absorption peaks correlated with observed in experimental measurements, was achieved.

C-dots interact in a more stable way with silver surface model of the AgNPs in dilute solutions though functional groups on C-dots surface. C-dots with a –COO group on its surface presents the higher interaction with the silver surface model. Due to the fact that -COOH is less stable than –COO on the silver surface model, it can be dissociated when it is adsorbed. Moreover, the presence of this group on C-dot

surfaces explains additional peaks features on UV-visible spectra for C-dots, and can be the responsible of its charge. In addition it is possible to predict a negative charge for the C-dots/AgNPs composite system interfaces, because C-dot is stably adsorbed.

Furthermore, in the case where D-glucose and D-gluconate ion capping agents are present, there is also an energetic preference of –COOH or –COO groups to replace D-glucose of the silver surface, yielding to an interaction between AgNPs and C-dots even in that special case.

Acknowledgments

The authors thank to ANPCyT (PICT-2016-4094). R.E. Ambrusi, M.E. Pronsato and A. Juan are members of CONICET and J.M. Arroyave is a Postdoctoral fellow of this institution. M.F. Pistonesi is a member of Comisión Investigaciones Científicas pcia. Bs. As. (CIC-BA).

References

[1] B.D. Pan, J. Zhang, Z. Li, and M. Wu, "Hydrothermal Route for Cutting Graphene Sheets into Blue-Luminescent Graphene Quantum Dots", Adv. Mater., vol. 22, 2010, pp. 734-738. DOI: 10.1002/adma.200902825.

[2] L. Zhi and K. Mullen, "A bottom-up approach from molecular nanographenes to unconventional carbon materials", J. Mater. Chem., vol. 18, 2008, pp. 1472-1484. DOI: 10.1039/b717585j.

[3] M. Zhao, F. Yang, Y. Xue, D. Xiao, and Y. Guo, "A Time-Dependent DFT Study of the Absorption and Fluorescence Properties of Graphene Quantum Dots", ChemPhysChem, vol. 15, 2014, pp. 950-957. DOI: 10.1002/cphc.201301137.

[4] J. Feng, H. Dong, Y. Liyan, and L. Dong, "Optical and Electronic Properties of Graphene Quantum Dots with Oxigen-Containing Groups: a Density Functional Theory Study", J. of Mater. Chem. C, vol. 5, 2017, pp. 5984-5993. DOI: 10.1039/C7TC00631D.

[5] D. Raeyani, S. Shojaei, and S. Ahmadi-Kandjani, "Optical Graphene Quantum Dots Gas Sensors: Theoretical Study", Superlattices and Microstructures, vol. 114, 2017, pp. 321-330. DOI: 10.1016/j.spmi.2017.12.050.

[6] P. Bugajny, L. Szulakowska, B. Jaworowski, and P. Potasz, "Optical properties of geometrically optimized graphene quantum dots", Physica E, vol. 85, 2017, pp. 294-301. DOI: 10.1016/j.physe.2016.08.030.

[7] A. Tiutiunnyk, C.A. Duque, F.J. Caro-Lopera, M.E. Mora-Ramos, and J.D. Correa, "Opto-electronic properties of twisted bilayer graphene quantum dots", Physica E: Low-dimensional Systems and Nanostructures, vol. 112, 2019, pp. 36-48. DOI: 10.1016/j.physe.2019.03.028.

[8] T. Pal, S. Mohiyuddin, and G. Packirisamy, "Facile and Green Synthesis of Multicolor Fluorescence Carbon Dots from Curcumin : In Vitro and in Vivo Bioimaging

and Other Applications", ACS Omega, vol. 3, 2018, pp. 831-843. DOI: 10.1021/acsomega.7b01323.

[9] Y. Wang, Y. Zhu, S. Yu, and C. Jiang, "Fluorescent carbon dots: rational synthesis, tunable optical properties and analytical applications", RSC Adv., vol. 7, 2017, pp. 40973-40989. DOI: 10.1039/C7RA07573A.

[10] W. Niu, Y. Li, R.Z. Dan Shan, Y. Fan, and X. Zhang, "Ethylenediamine-Assisted Hydrothermal Synthesis of Nitrogen-Doped Carbon Quantum Dots as Fluorescent Probes for Sensitive Biosensing and Bioimaging", Sensors and Actuators B: Chemical, vol. 218, 2015, pp. 229-236. DOI: 10.1016/j.snb.2015.05.006.

[11] L. Zheng, Y. Chi, Y. Dong, J. Lin, and B. Wang, "Electrochemiluminescence of Water-Soluble Carbon Nanocrystals Released Electrochemically from Graphite", J. Am. Chem. Soc., vol. 131, 2009, pp. 4564-4565. DOI: 10.1021/ja809073f CCC.

[12] W. Xue, Z. Lin, H. Chen, C. Lu, and J. Lin, "Enhancement of Ultraweak Chemiluminescence from Reaction of Hydrogen Peroxide and Bisulfite by Water-Soluble Carbon Nanodots", J. Phys. Chem. C, vol. 115, 2011, pp. 21707-21714. DOI: 10.1021/jp207554t.

[13] S.N. Baker and G.A. Baker, "Luminescent Carbon Nanodots: Emergent Nanolights", Angewandte Chemie, vol. 49, 2010, pp. 6726 - 6744. DOI: 10.1002/anie.200906623.

[14] B. Gao, Y. Tang, H. Sun, Y. Xuan, L. Xu, and C. Huang, "A label-free and turn-on fluorescence sensor for sensitive and selective detection of iodide using carbon nanodots/silver nanocomposites", Anal. Methods, vol. 7, 2015, pp. 4038-4043. DOI: 10.1039/C4AY03092C.

[15] D. Jiang, Y. Zhang, M. Huang, J. Liu, J. Wan, H. Chu, and M. Chen, "Carbon nanodots as reductant and stabilizer for one-pot sonochemical synthesis of amorphous carbon-supported silver nanoparticles for electrochemical nonenzymatic H2O2 sensing", J. of Electroanal.Chem., vol. 728, 2014, pp. 26-33. DOI: 10.1016/j.jelechem.2014.06.017.

[16] J. Ma, B. Yin, X. Wu, and B. Ye, "Simple and Cost-Effective Glucose Detection Based on Carbon Nanodots Supported on Silver Nanoparticles", Anal. Chem., vol. 89, 2017, p. 1323–1328. DOI: 10.1021/acs.analchem.6b04259.

[17] M. Liu and W. Chen, "Green synthesis of silver nanoclusters supported on carbon nanodots: enhanced photoluminescence and high catalytic activity for oxygen reduction reaction", Nanoscale, vol. 5, 2013, pp. 12558-12564. DOI: 10.1039/c3nr04054b.

[18] H. Liu, Z. Li, Y. Sun, X. Geng, Y. Hu, H. Meng, J. Ge, and L. Qu, "Synthesis of Luminescent Carbon Dots with Ultrahigh Quantum Yield and Inherent Folate Receptor-Positive Cancer Cell Targetability", Scientific Reports, vol. 8, 2018, pp. 1-8. DOI: 10.1038/s41598-018-19373-3.

[19] Y. Lu, N. Li, L. Jia, R. Ma, W. Jia, X. Tao, H. Cui, and H. Wang, "The synthesis of Ag@CQDs composite and its electrochemiluminescence application for the highly selective and sensitive detection of chloride", J of Electroanal. Chem., vol. 781, 2016, pp. 114-119. DOI: 10.1016/j.jelechem.2016.05.045.

[20] A.J. González Fá, A. Juan, and M.S. Di Nezio, "Synthesis and Characterization of Silver Nanoparticles Prepared with Honey: The Role of Carbohydrates", Anal. Lett., vol. 50, 2017, pp. 877-888. DOI: 10.1080/00032719.2016.1199558.

[21] A. González Fá, I. López-Corral, R. Faccio, A. Juan, and M.S. Di Nezio, "Surface enhancement Raman spectroscopy and density functional theory study of silver nanoparticles synthetized with D-glucose", J. Raman Spectrosc., vol. 49, 2018, pp. 1-9. DOI: 10.1002/jrs.5466.

[22] T. Yoshinaga, Y. Iso, and T. Isobe, "Particulate, Structural, and Optical Properties of D-Glucose-Derived Carbon Dots Synthesized by Microwave-Assisted Hydrothermal Treatment", J. of Solid Science and Technology, vol. 7, 2018, pp. 3034-3039. DOI: 10.1149/2.0091801jss.

[23] G. Kresse and J. Furthmuller, "Efficient iterative schemes for ab initio total-energy calculations using a plane-wave basis set", Phys. Rev. B, vol. 54, 1996, pp. 11169-11186.

[24] G. Kresse and J. Furthmüller, "Efficiency of ab-initio total energy calculations for metals and semiconductors using a plane-wave basis set", Comput. Mater. Sci., vol. 6, 1996, pp. 15-50.

[25] J.P. Perdew, K. Burke, and M. Ernzerhof, "Generalized gradient approximation made simple, Phys", Phys. Rev. Lett., vol. 77, 1996, pp. 3865-3868.

[26] P.E. Blochl, "Projector augmented wave method", Phys. Rev. B, vol. 50, 1994, pp. 17953-17979.

[27] G. Kresse and D. Joubert, "From ultrasoft pseudopotentials to the projector augmented-wave method", Phys. Rev. B, vol. 59, 1999, pp. 1758-1775.

[28] H.J. Monkhorst and J.D. Pack, "Special points for Brillonin-zone integrations", Phys. Rev. B, vol. 13, 1976, pp. 5188-5192.

[29] W.H. Press, S.A. Teukolsky, W.T. Vetterling, and B.P. Flannery, Numerical Recipes, Cambridge University Press, New York, 1986.

[30] S. Grimme, "Semiempirical GGA-Type Density Functional Constructed with a Long-Range Dispersion Correction", J. Comput. Chem., vol. 27, 2006, pp. 1787-1799. DOI: 10.1002/jcc.

[31] J. Paier, M. Marsman, G. Kresse, J. Paier, M. Marsman, and G. Kresse, "Why does the B3LYP hybrid functional fail for metals ?", J. Chem. Phys., vol. 127, 2007, p. 024103. DOI: 10.1063/1.2747249.

[32] K. Mathew and R.G. Hennig, "Implicit self-consistent description of electrolyte in plane-wave density-functional theory", 2016, pp. 1-6. Publisher: arXiv:1601.03346v1 [cond-mat.mtrl-sci].

[33] K. Mathew, R. Sundararaman, K. Letchworth-weaver, T.A. Arias, and R.G. Hennig, "Implicit solvation model for density-functional study of nanocrystal surfaces and reaction pathways", J Chem. Phys., vol. 140, 2014, p. 084106. DOI: 10.1063/1.4865107.

[34] T.N. Rekha and B.J. Rajkumar, "Density functional theory study on silver clusters using dimers , trimers , and tetramers as building units", Can. J. Phys., vol. 93, 2015, pp. 1-8. DOI: 10.1139/cjp-2014-0256.

[35] A. Parameswari, R.M. Asath, R. Premkumar, and A.M. Benial, "SERS and quantum chemical studies on N-methylglycine molecule on silver nanoparticles", J. of Molecular Structure, vol. 1138, 2017, pp. 102-109. DOI: 10.1016/j.molstruc.2017.03.014.

[36] R. Fournier, "Theoretical study of the structure of silver clusters", J. of Chem. Phys., vol. 115, 2001, pp. 2165-2177. DOI: 10.1063/1.1383288.

[37] M. Gajdoš, K. Hummer, G. Kresse, J. Furthmüller, and F. Bechstedt, "Linear optical properties in the projector-augmented wave methodology", Phys. Rev. B, vol. 73, 2006, p. 045112. DOI: 10.1103/PhysRevB.73.045112.

[38] S. Baroni and R. Resta, "Ab initio calculation of the macroscopic dielectric constant in silicon", Phys. Rev. B, vol. 33, 1986, pp. 7017-7021.

[39] Y. Choi, Y. Choi, O. Kwon, and B. Kim, "Carbon Dots: Bottom-Up Syntheses, Properties, and Light- Harvesting Applications", Chemistry- An Asian Journal, vol. 13, 2018, pp. 586-598. DOI: 10.1002/asia.201701736.

[40] M. Cui, S. Ren, H. Zhao, L. Wang, and Q. Xue, "Novel nitrogen doped carbon dots for corrosion inhibition of carbon steel in 1 M HCl solution", Appl. Surf. Sci., vol. 443, 2018, pp. 145-156. DOI: 10.1016/j.apsusc.2018.02.255.

[41] X. Sun and Y. Li, "Colloidal Carbon Spheres and Their Core/Shell Structures with Noble-Metal Nanoparticles", Angew. Chem. Int. Ed., vol. 43, 2004, pp. 597 -601. DOI: 10.1002/anie.200352386.

[42] N. Ooi, A. Rairkar, and J.B. Adams, "Density functional study of graphite bulk and surface properties", Carbon, vol. 44, 2006, pp. 231-242. DOI: 10.1016/j.carbon.2005.07.036.

[43] P. Atkins and R. Friedman, Molecular quantum Mechanics, Fourth Edition, Oxford University Press, Oxford, 2005.

[44] K. Sakamoto, N. Nishina, T. Enoki, and J. Aihara, "Aromatic Character of Nanographene Model Compounds", J. of Phys. Chem. A, vol. 118, 2014, pp. 3014-3025. DOI: 10.1021/jp5017032.

[45] S. Fujii and T. Enoki, "Nanographene and Graphene Edges: Electronic Structure and Nanofabrication", Acc. Chem. Res., vol. 46, 2013, pp. 2202-2210. DOI: 10.1021/ar300120y.

[46] A.D. Zdetsis and E.N. Economou, "Electronic and Aromatic properties of Graphene and Nanographenes of various kinds: New Insights and Results", Adv. Mater. Lett., vol. 8, 2017, pp. 02-07. DOI: 10.5185/amlett.2016.7104.

[47] S. Xie, R. Huang, and L. Zheng, "Separation and identification of perchlorinated polycyclic aromatic hydrocarbons by high-performance liquid chromatography and ultraviolet absorption spectroscopy", J. of Chromatogr. A, vol. 864, 1999, pp. 173-177.

[48] M. Li, W. Li, and S. Liu, "Control of the morphology and chemical properties of carbon spheres prepared from glucose by a hydrothermal method", J. Mater. Res., vol. 27, 2012, pp. 1117-1123. DOI: 10.1557/jmr.2011.447.

[49] M. Sevilla and A.B. Fuertes, "Chemical and structural properties of carbonaceous products obtained by hydrothermal carbonization of saccharides", Chem. Eur. J., vol. 15, 2009, pp. 4195-4203. DOI: 10.1002/chem.200802097.

[50] A. González Fa, Synthesis and characterization of metallic nanoparticles obtained from honey, PhD Thesis, Universidad Nacional del Sur, 2017.

[51] K.L. Kelly, E. Coronado, L.L. Zhao, and G.C. Schatz, "The Optical Properties of Metal Nanoparticles: The Influence of Size, Shape, and Dielectric Environment", J. Phys. Chem. B, vol. 107, 2003, pp. 668-677. DOI: 10.1021/jp026731y.

[52] J.E. Millstone, S.J. Hurst, G.S. Metraux, J.I. Cutler, and C.A. Mirkin, "Colloidal Gold and Silver Triangular Nanoprisms", Nano Micro Small, vol. 5, 2009, pp. 646-664. DOI: 10.1002/smll.200801480.

[53] C. Cohen-Tannoudji, B. Diu, and F. Laloe, Quantum Mechanics, vol. 2, WILEY-VCH, New Jersey, 1986.

[54] J. Harl, The linear response function in density functional theory: Optical spectra and improved description of electron correlation, PhD Thesis, universitat Wien, 2008.

Journal: Physica E: Low-dimensional Systems and Nanostructures

Ref. No: PHYSE_2019_672

Title: Density Functional Theory model for carbon dot surfaces and their interaction with silver nanoparticles

Author(s): R.E. Ambrusi, J.M. Arroyave, M.E. Centurión, M.S. Di Nezio, M.F. Pistonesi, A. Juan, M.E. Pronsato.

The authors of the present work ensure that there is not conflict of interest.